Phys Chem Minerals (2004) 31: 269–277
DOI 10.1007/s00269-004-0384-0

ORIGINAL PAPER

A-L. Auzende · I. Daniel · B. Reynard · C. Lemaire
F. Guyot

High-pressure behaviour of serpentine minerals: a Raman spectroscopic study

Received : 23 April 2002 / Accepted : 5 January 2004

Abstract Four main serpentine varieties can be distinguished on the basis of their microstructures, *i.e.* lizardite, antigorite, chrysotile and polygonal serpentine. Among these, antigorite is the variety stable under high pressure. In order to understand the structural response of these varieties to pressure, we studied well-characterized serpentine samples by *in situ* Raman spectroscopy up to 10 GPa, in a diamond-anvil cell. All serpentine varieties can be metastably compressed up to 10 GPa at room temperature without the occurrence of phase transition or amorphization. All spectroscopic pressure-induced changes are fully reversible upon decompression. The vibrational frequencies of antigorite have a slightly larger pressure dependence than those of the other varieties. The O–H-stretching modes of the four varieties have a positive pressure dependence, which indicates that there is no enhancement of hydrogen bonding in serpentine minerals at high pressure. Serpentine minerals display two types of hydroxyl groups in the structure: inner OH groups lie at the centre of each six-fold ring while outer OH groups are considered to link the octahedral sheet of a given 1:1 layer to the tetrahedral sheet of the adjacent 1:1 layer. On the basis of the contrasting behaviour of the Raman bands as a function of pressure, we propose a new assignment of the OH-stretching bands. The strongly pressure-dependent modes are assigned to the vibrations of the outer hydroxyl groups, the less pressure-sensitive peaks to the inner ones.

Keywords Raman spectroscopy · High pressure · Serpentine minerals · Diamond-anvil cell

A.-L. Auzende
Laboratoire Magmas et Volcans, UMR 6524,
CNRS-UBP-OPGC, 5, rue Kessler,
63038 Clermont-Ferrand cedex

I. Daniel (✉) · B. Reynard
Laboratoire de Sciences de la Terre, UMR 5570,
CNRS-UCBL-ENSL, 43 bd du 11 novembre,
69622 Villeurbanne cedex and 46 Allée d'Italie,
69364 Lyon cedex 07
e-mail: Isabelle.Daniel@univ-lyon1.fr
Tel: +33 4 72 44 62 35
Fax: +33 4 72 44 85 93

C. Lemaire · F. Guyot
Laboratoire de Minéralogie-Cristallographie de Paris,
UMR 7590, CNRS-UP VI and VII and IPGP, 4,
place Jussieu, 75252 Paris cedex 05

Introduction

Serpentine minerals are hydrous phyllosilicates (~13 wt% water) formed during the hydration of basic and ultrabasic rocks. Serpentine minerals are rather abundant in the oceanic lithosphere, conferring on them an important role in the global water cycle (Scambelluri et al. 1995; Ulmer and Trommsdorff 1995; Wunder and Schreyer 1997; Iwamori 1998; Schmidt and Poli 1998).

Serpentine minerals are based upon a 1:1 layer structure, corresponding to the stacking of layers composed of one tetrahedral and one octahedral sheet (Fig. 1). Changes in the curvature of these 1:1 layers lead to four distinct varieties (*e.g.* Wicks and O'Hanley 1988). Lizardite displays a planar structure, chrysotile a cylindrical wrapping of the 1:1 layers, leading to its fibrous habit (asbestos), and antigorite is characterized by a modulated structure involving also changes in the layer polarity. Finally, polygonal serpentine alternates flat and curved sectors and has a fibrous habit like chrysotile (*e.g.* Baronnet et al. 1994). Recent experimental studies have shown that among serpentine minerals, antigorite is the variety stable under high-pressure conditions (Bose and Ganguly 1995; Ulmer and Trommsdorff 1995; Wunder and Schreyer 1997). Moreover, natural serpentinites sampled in high-grade terrains also display antigorite as the most abundant variety in the matrix (Mellini et al. 1987; Scambelluri et al. 1995; Guillot et al. 2000; Auzende et al. 2002). Lizardite and chrysotile are the major components of pseudomorphic textures

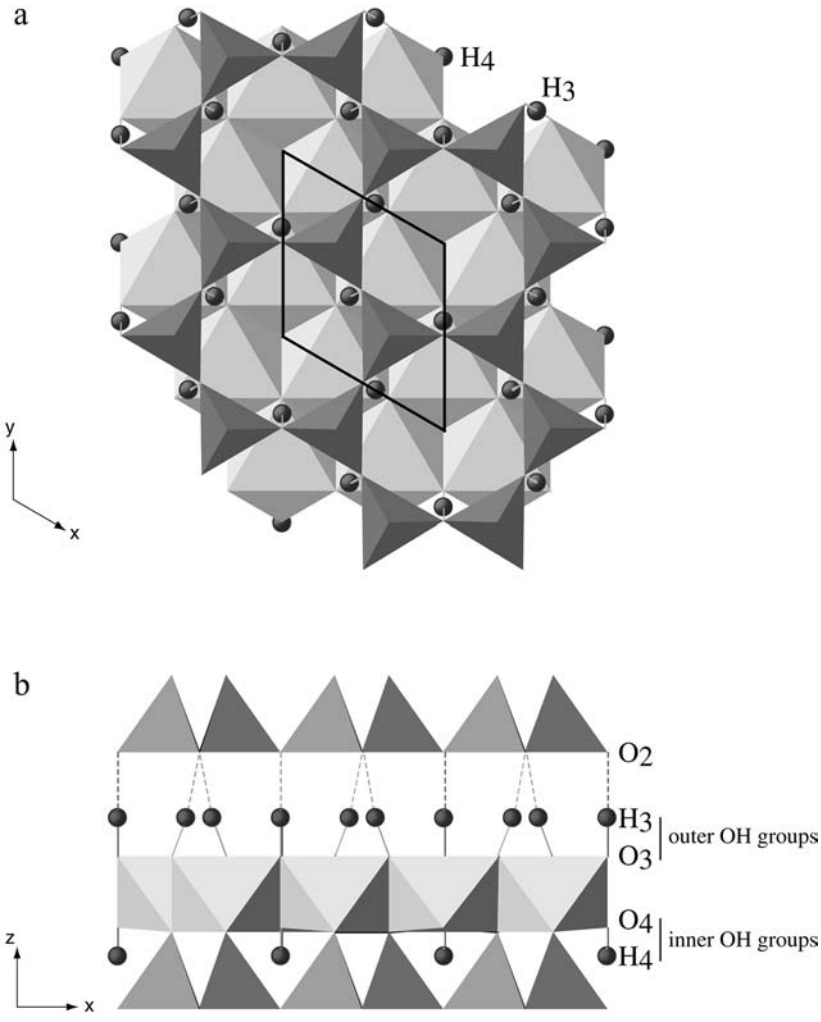

Fig. 1 a, b Crystal structure of lizardite-1*T* (Mellini 1982). **a** View along [001] and **b** view along [010]. O4–H4 corresponds to the inner OH groups and O3–H3 to the outer OH groups. *T* is the tetrahedral sheet and *O* the octahedral one

observed in low-grade serpentinites such as those found in oceanic lithosphere or low metamorphic grade ophiolites. Hence, in order to understand the contrasting behaviour of the various serpentine varieties with respect to pressure, we investigated their behaviour up to 10 GPa. The results point out that antigorite is slightly more sensitive to pressure than the other varieties and provide new constraints on the still-debated assignment of the OH-stretching vibrational modes.

Experimental

Sample characterization

This study was performed on well-characterized natural samples, even though simultaneous occurrence of several phases is often observed in serpentinites (Viti and Mellini 1997). The chemical analyses and structural formulae are given in Table 1. These samples are close to the ideal formula $Mg_3Si_2O_5(OH)_4$, with only slight substitutions of Mg and Si by Fe and Al, respectively.

The lizardite sample comes from Monte-Fico (Isle of Elba). The structure and chemistry of this material have been extensively investigated (Mellini and Viti 1994; Fuchs et al. 1998). The sample occurs as a polycrystalline material. Lizardite crystals occur as trigonal prisms, typically $0.3 \times 0.3 \times 0.7$ mm in size. They correspond to the 1*T* polytype, which is the closest to the ideal serpentine trigonal structure. Lizardite 1*T* displays only small distortions of the tetrahedral layer, and was refined in space group *P*31*m* (Mellini and Viti 1994). The structural formulae (Table 1) indicate that the lizardite is more substituted in Fe and Al than chrysotile and polygonal serpentine, in agreement with the results of the

Table 1 Microprobe analyses of the investigated serpentine samples and associated structural formulae

	Lizardite[a]	Chrysotile[b]	Polygonal[c]	Antigorite[c]
SiO_2	39.60	43.50	43.20	41.65
Al_2O_3	2.90	0.60	0.80	3.45
FeO	3.84	2.60	2.30	4.15
MgO	38.00	38.80	40.60	37.37
Total	84.34	85.50	86.9	86.66
Si	1.92	2.06	2.01	1.96
Al	0.17	0.03	0.04	0.19
Fe	0.16	0.10	0.09	0.16
Mg	2.75	2.73	2.82	2.62
Total	4.99	4.93	4.97	4.94

[a] Mellini and Viti (1994)
[b] Fuchs et al. (1998)
[c] this study

chemical investigations of Wicks and Whittaker (1970). However, it contains less aluminium than antigorite. Although observations both by optical microscopy and by transmission electron microscopy (TEM) revealed minor amounts of chrysotile (less than 5%), lizardite is the dominant mineral in the sample (Viti and Mellini 1997).

The antigorite sample originates from the Escambray Massif (Central Cuba). It occurs as a polycrystalline aggregate where antigorite blades are several tenths of a mm in size. Antigorite is considered to be monoclinic (*e.g.* Wicks and O'Hanley 1988), and has been tentatively assigned to space group *Pm* (Uehara 1998), although no three-dimensional refinement can precisely constrain its structure. The crystals are mostly one-layer polytypes, with a regular superperiodicity of 37 Å ($m = 13$) and fine stacking sequences (Auzende et al. 2002). The antigorite sample displays substitutions in Fe and Al reaching 4.2 and 3.5 wt%, respectively. TEM observations have indicated that this sample consists mostly of antigorite, associated with minor amounts of chrysotile (less than 5%) (Auzende et al. 2002).

The fibrous varieties, *i.e.* chrysotile and polygonal serpentine, display similar substitution rates, with small amounts of Fe ($< 3\%$) and Al ($< 1\%$) in the structure. The chrysotile sample originates from the asbestos mines of Thetford (Quebec). It consists of a black compact serpentinite associated with white fibrous veins. The fibres used had been previously characterized by X-ray diffraction (Lemaire et al. 1999), and correspond to the monoclinic polytype (clinochrysotile). Their characteristic diameter is 100 nm. The polygonal serpentine sample comes from the Jeffrey Mines (Quebec). The TEM study revealed a combination of polygonal serpentine fibres larger than 200 nm, and a small amount of chrysotile (less than 5%).

High pressure techniques

High-pressure experiments were performed in a Mao-Bell-type diamond-anvil cell, equipped with 600-μm culet low fluorescence diamonds; 200 μm-diameter holes drilled in a stainless-steel gasket pre-indented at ~80 μm thickness served as pressure chambers. The samples were cut with a razor blade to approximately 30 μm thickness. A 16:3:1 methanol–ethanol–water mixture was used as a pressure-transmitting medium to achieve hydrostatic conditions to 10 GPa, at room temperature. Pressure was determined by the calibrated shift of the R1 fluorescence line of a ruby chip located next to the sample (Mao et al. 1986). Raman spectra were recorded in the backscattered geometry, with a Dilor XY double subtractive spectrograph equipped with 1800 g mm^{-1} holographic gratings, and a nitrogen liquid-cooled EGG CCD detector. The resolution was 1 cm^{-1}. A microscope with a Mitutoyo Apoplan 50x long-working distance objective was used to focus the incident laser beam (514.5 nm line of an Ar^+ laser) into a 2-μm spot and to collect the Raman signal from the sample. Spectra were acquired over 120 to 600 s, with a laser output power adjusted between 200 and 600 mW depending on the intensity of the signal.

Fitting procedure

In the low-frequency range (200–800 cm^{-1}), adjustments of the spectra by Voigt functions make it possible to get the peak positions and the full width at half maximum (FWHM). Since the signal is rather complex in the O–H-stretching region, the different O–H-contributions were deconvoluted using Voigt functions. Fitting models were created from high-pressure spectra, where the Raman bands are best resolved due to a large splitting, difference from room condition, where bands are highly convoluted. We chose the minimum number of peaks required to gain the best fit to the spectra. These peaks were allowed to vary only in position and intensity, working from high to low pressure.

Results

Raman spectra of lizardite, antigorite, chrysotile and polygonal serpentine were recorded *in situ* upon compression to peak pressures of 9.5, 11.3, 7.1 and 10.8 GPa, respectively, then along the decompression path. Selected Raman spectra collected at various pressures in the low-(200–800 cm^{-1}) and high-(3550–3850 cm^{-1}) frequency ranges are displayed in Fig. 2. The investigated pressure range embraces the pressure stability field of antigorite (Ulmer and Trommsdorff 1995), *i.e.* the serpentine variety stable at high pressure. Only chrysotile could not be investigated above 7.1 GPa. Indeed, at 8.0 GPa, we could neither observe the sample in the DAC nor focus the laser beam onto it, suggesting that chrysotile and the pressure-transmitting medium had reached the same refractive index. Upon decompression, the chrysotile sample recovered both contrast and Raman spectrum, without any noticeable change in the spectrum. The evolution of all bands as a function of pressure is fully reversible, as indicated by the similar data obtained upon compression and decompression (Fig. 3).

Under ambient conditions, the Raman spectra characteristics of the four serpentine varieties are in excellent agreement with those described by Lemaire et al. (1999). The low-frequency Raman signal of the four different varieties, corresponding to lattice and internal vibrational modes, is almost identical (Fig. 2). Nevertheless, some slight differences distinguish one variety from the other. While lizardite displays a very weak Raman peak at 240 cm^{-1}, this mode is more intense in the spectra of the other varieties, and occurs around 230 cm^{-1}. In this frequency range, the Raman modes at 390, 433, 465 and 624 cm^{-1} are identical for lizardite, chrysotile and polygonal serpentine, but are systematically shifted toward lower frequencies in the antigorite Raman spectra. Hence, antigorite and lizardite can be easily distinguished from the fibrous varieties, on the basis of their Raman spectrum at low-frequency. In the high-frequency domain (3550–3850 cm^{-1}), the vibrational signal corresponds to the internal stretching vibrations of the OH groups. Lizardite displays two intense peaks at 3688 and 3703 cm^{-1}. Chrysotile shows a major peak at 3699 cm^{-1} with a shoulder at 3685 cm^{-1}. Polygonal serpentine has a signal intermediate between chrysotile and lizardite (Lemaire et al. 1999) with a major peak at 3695 cm^{-1} and a shoulder at 3688 cm^{-1}. These three varieties also display a very weak peak centred around 3650 cm^{-1}. The signal displayed by antigorite is decomposed in two major bands centred at 3665 and 3697 cm^{-1} and a weak band at 3619 cm^{-1}. The large differences in band positions permit a good discrimination between the four structural varieties (Lemaire et al. 1999).

Upon compression, all Raman bands shift toward higher wavenumbers (Fig. 2). In antigorite spectra, for instance, these shifts are comparable for all peaks in the low-frequency range, whereas they display a contrasting

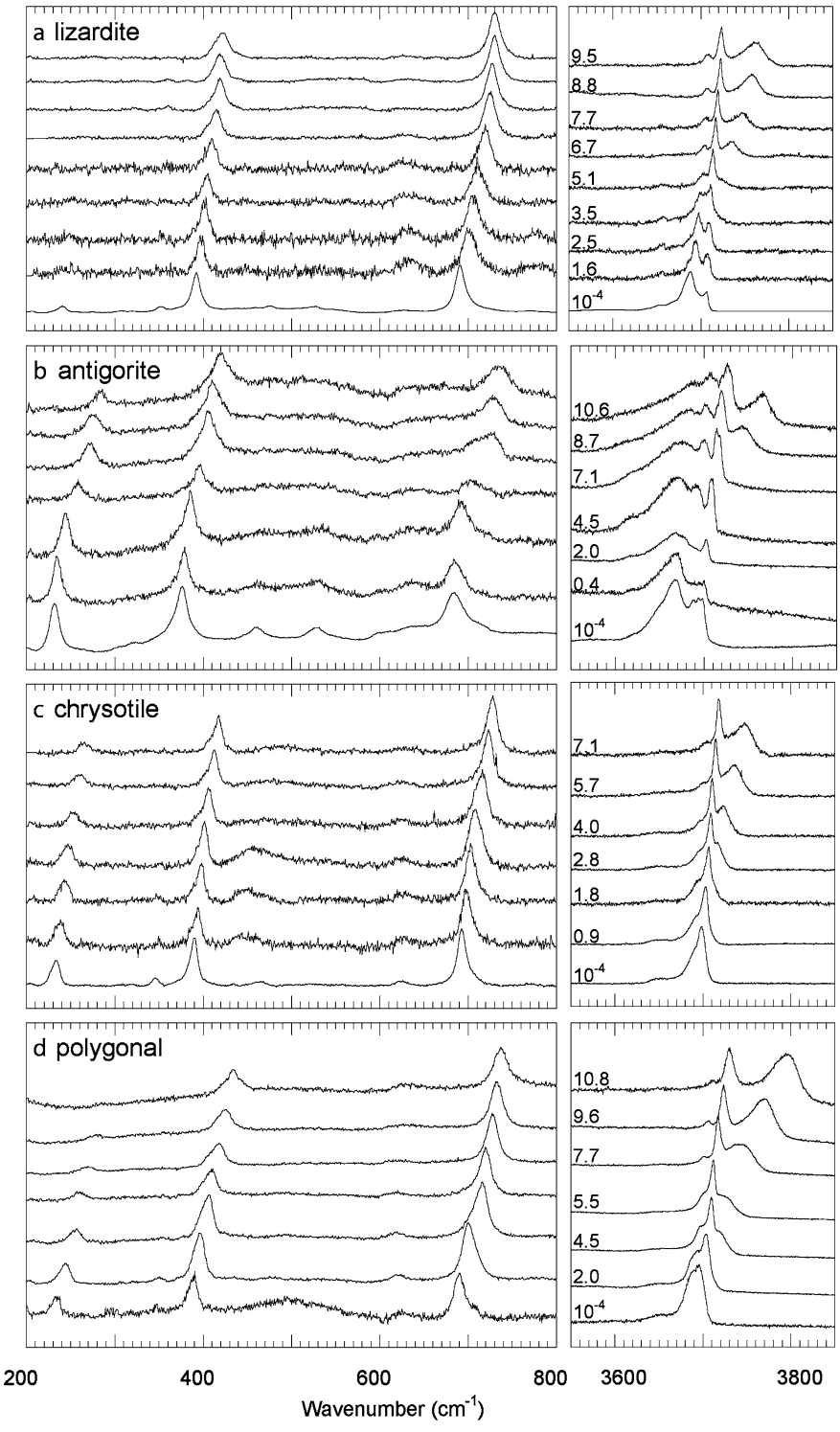

Fig. 2 **a–d** Reduced (*i.e.* with intensity corrected for first-order frequency dependence) Raman spectra of serpentine minerals at ambient temperature under increasing pressure. **a** lizardite; **b** antigorite; **c** chrysotile; **d** polygonal serpentine

behaviour at high frequency. The Raman band located at 3699 cm^{-1} under ambient conditions is shifted to 3730 cm^{-1} at 10.6 GPa, while the band centred at 3665 cm^{-1} is shifted to 3770 cm^{-1} over the same pressure range. These features, *i.e.* a similar behaviour in the low-frequency range and contrasted shift rates in the OH-stretching range, are shared by all serpentine varieties (Fig. 2).

The pressure evolution of all measured frequencies is plotted in Fig. 3. Only intense bands could be followed upon increasing pressure. Weak bands under ambient conditions rapidly lose resolution (*e.g.* the peak at 461 cm^{-1} in antigorite spectra). Linear regressions were used to fit the frequencies of the lattice and internal vibration modes (from 200 to 800 cm^{-1}) as a function of pressure (Table 2). They display with a mean slope

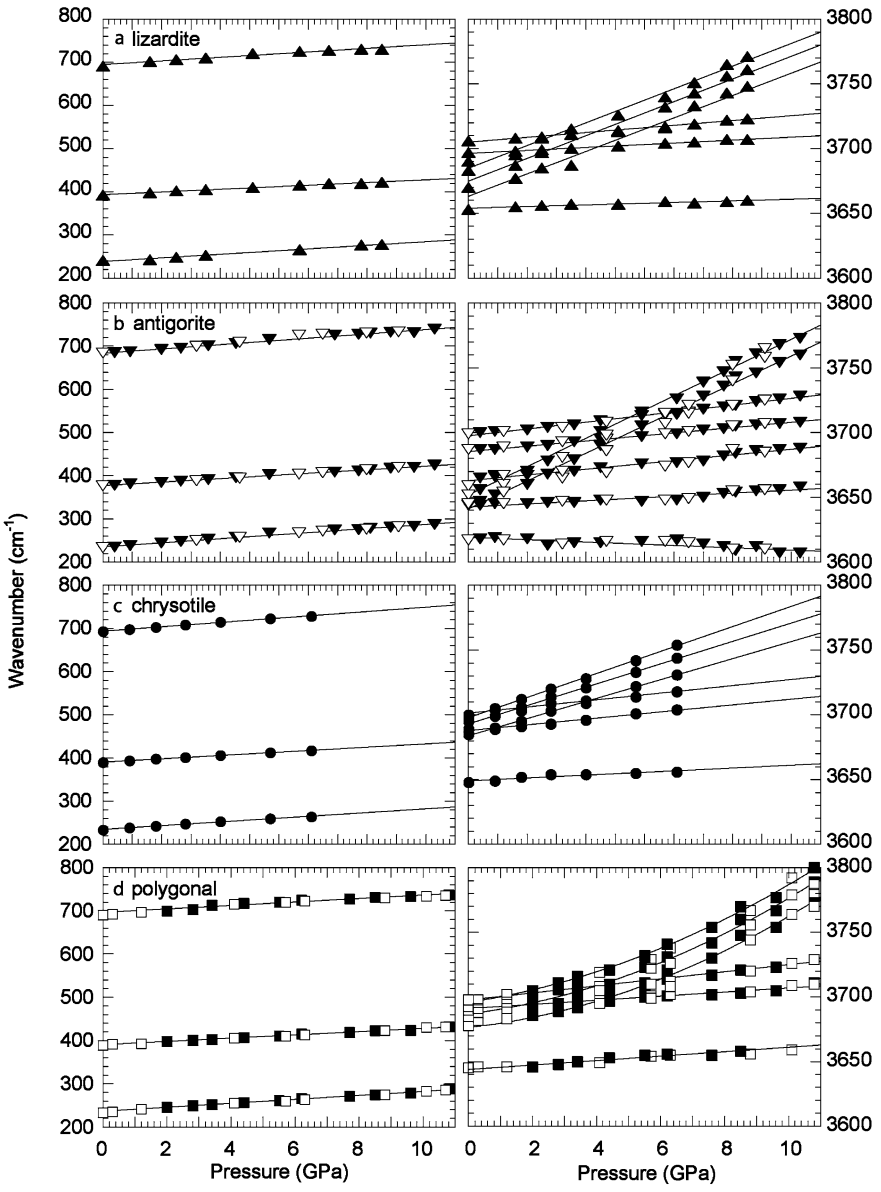

Fig. 3 a–d Pressure dependence of the Raman mode frequencies. *Full symbols* represent data obtained during compression and *empty symbols* correspond to decompression data. *Symbol size* exceeds the estimated standard deviations in the pressure estimation and frequencies. **a** Lizardite; **b** antigorite; **c** chrysotile; **d** polygonal serpentine

Table 2 Observed Raman modes for the low-pressure spectra and their pressure dependence obtained as linear fits to data. The error on the slope is given in brackets. In the case of polygonal serpentine three bands were fitted with polynomial curve fits of the form $y = ax + bx + c$

Lizardite		Chrysolite		Antigorite		Polygonal		
v_0 (cm^{-1})	dv/dP (cm^{-1} GPa^{-1})	v_0 (cm^{-1})	dv/dP ($cm^{-1}GPa^{-1}$)	v_0 (cm^{-1})	dv/dP ($cm^{-1}GPa^{-1}$)	v_0 (cm^{-1})	dv/dP ($cm^{-1}GPa^{-1}$)	dv^2/dP^2 ($cm^{-1}GPa^{-1}$)
238	4.2(2)	235	4.3(2)	235	4.8(2)	236	4.6(1)	
393	3.1(1)	391	3.9(1)	377	4.1(1)	391	3.7(1)	
695	4.1(3)	694	5.0(2)	685	4.9(2)	696	4.0(3)	
				3619	−0.9(2)			
3654	0.7(1)	3649	1.1(2)	3641	1.2(1)	3646	1.4(2)	
3670	8.6(5)	3684	6.6(2)	3643	10.8(2)	3678	10.5(1)[a]	1.18
3683	8.8(5)	3689	2.2(1)	3652	10.9(3)	3685	10.5(2)[a]	1.19
3690	8.8(3)	3694	7.1(3)	3661	2.3(1)	3690	10.1(1)[a]	1.06
3697	1.1(1)	3698	7.8(1)	3686	2.1(1)	3691	1.6(1)	
3706	1.9(1)	3701	2.4(1)	3698	2.6(1)	3698	2.7(1)	

[a] Mean slope over the considered pressure range

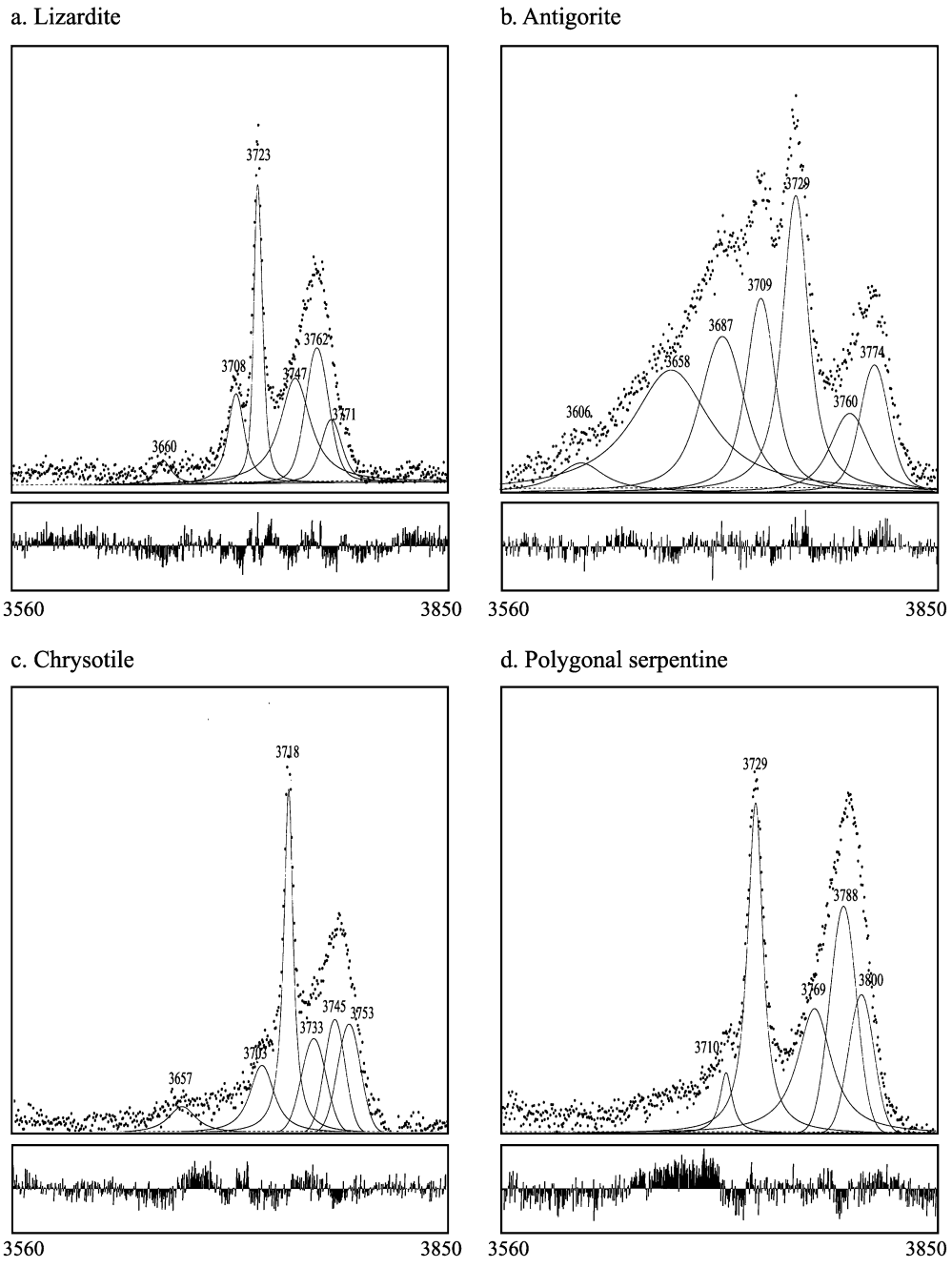

Fig. 4 a–d Deconvolution of the Raman signal in the O–H-stretching mode area and associated fitting residues at 9.5, 11.3, 7.1 and 10.8 GPa for **a** lizardite **b** antigorite **c** chrysotile and **d** polygonal serpentine, respectively. The band, which is located at 3646 cm^{-1} in polygonal serpentines under ambient conditions, is not resolved in the 10.8 GPa spectrum

$(\partial v/\partial P)_T = 4.2(2)\,cm^{-1}\,GPa^{-1}$. Antigorite vibrations are characterized by a pressure dependence $(\partial v/\partial P)_T = 4.6(2)\,cm^{-1}\,GPa^{-1}$ slightly higher than those of the other serpentine varieties. No significant correlation of the FWHM of the lattice modes with pressure has been evidenced in this study. For example, the FWHM of the 230 cm^{-1} band of antigorite is 13(1) cm^{-1} under ambient conditions, 15(2) cm^{-1} at 4.5 GPa and 14(2) cm^{-1} at 7.8 GPa. This confirms that serpentine minerals do not tend to amorphize within the investigated pressure range, and that pressure conditions were kept hydrostatic along the different experiments.

In the high-frequency range (3550–3850 cm^{-1}), six active Raman OH-stretching bands are used to deconvolute the spectra of lizardite, chrysotile and polygonal serpentine, while seven bands are required to best fit the signal of antigorite (Fig. 4). The bandwidths extend from 10 to 25 cm^{-1} for all but one band. Indeed, the band centred at 3658 cm^{-1} in the antigorite high-pressure spectrum (Fig. 4) is poorly resolved and its high FWHM (64 cm^{-1}) strongly suggests that it contains several unresolved peaks.

The bands in the 3550–3850 cm^{-1} range display a positive linear dependence on pressure, except three bands of the polygonal serpentine (Fig. 3), whose pressure evolution is best fitted by a second-order polynomial relationship. For all varieties, two distinct behaviours are recognized in this frequency domain:

strongly pressure-dependent bands with positive shift rates between 6.6 and 10.9 cm^{-1} GPa^{-1} and weakly pressure-dependent peaks with shift rates between 1.1 and 2.7 cm^{-1} GPa^{-1}. The bands displaying the larger pressure dependences are those located on the low-frequency side at ambient conditions. With increasing pressure, these bands catch up and then overrun the sluggish bands. As already observed in the low-frequency domain, the most pressure-sensitive bands in the O–H-stretching region belong to antigorite. The weak bands centred around 3650 cm^{-1} in lizardite, chrysotile and polygonal serpentine display lower shifting rates than antigorite (Table 2). Antigorite spectra also display a weak peak (3619 cm^{-1} under ambient conditions) with a slightly negative shift (Table 2). This peak was not documented in the spectra of the other varieties.

Discussion

Pressure-induced changes in serpentine minerals

When compressed, the serpentine varieties (lizardite, antigorite, chrysotile and polygonal serpentine) still display well-resolved Raman spectra close to 10 GPa and room temperature, thus indicating no amorphization of serpentine minerals up to this pressure, in agreement with Irifune et al. (1996), who did not detect the amorphization of antigorite or lizardite up to 26 GPa at room temperature. In the opposite, Meade and Jeanloz (1991) described a gradual amorphization of serpentine in a pressure interval between 6 to 22 GPa, probably due to large non-hydrostatic stresses in their experiments, in which no pressure-transmitting medium was used.

The continuous shifts and the absence of modification in the number of peaks over the whole spectral range (Fig. 2 and 3), indicate that lizardite, antigorite and chrysotile do not undergo any phase transition to 10 GPa. Upon increasing pressure, vibrational frequencies corresponding to lattice and internal tetrahedral layer modes move to higher wavenumbers. Hence, albeit the arrangement of the 1 : 1 layers is different from one serpentine to the other, leading to the four structural varieties, the layers compress in a closely related way. Antigorite Raman bands display slightly but significantly larger shift rates of the modes observed below 1000 cm^{-1} than in chrysotile and lizardite (Table 2). These bands are attributed to metal–oxygen vibrations (around 230 cm^{-1}) and to a combination of internal vibration modes (between 350 and 800 cm^{-1}) within the 1:1 layer (*e.g.* Kloprogge et al. 1999). Since all Raman modes of antigorite display a slightly but significantly higher pressure dependence than those of the other varieties, it might suggest a larger compressibility of this serpentine variety, although this would have to be confirmed by a *PV* equation of state of serpentine minerals.

In the high-frequency range, the different O–H contributions were deconvoluted using Voigt functions. The number of peaks accepted to fit the spectra derives in part from structural data. In serpentine minerals, there exist two independent OH groups (Fig. 1). The inner hydroxyl groups O4H4 lie at the centre of each six-fold ring at the same *z* level as the apical oxygen O_2 (*e.g.* Wicks and O'Hanley 1988). These hydroxyls are not involved in bonds with surrounding oxygen atoms. The outer OH groups O3H3 are considered to link the octahedral sheet of a given 1:1 layer to the tetrahedral sheet of the adjacent 1:1 layer. Balan et al. (2002) argued that three IR absorption bands occur in the range of O–H-stretching bands of lizardite 1*T*. The lizardite 1*T* structure, refined in $P31m$, belongs to the $C3v$ factor group. In this group, the four OH groups of the subcell give four stretching modes: two symmetric modes A1 (inner OH stretch and in-phase stretch of outer OH) and two degenerated (out-of-phase stretch of outer OH). For the other varieties, more than four bands can be expected, as the symmetry decreases. Finally, if we consider the antigorite supercell, a higher number of bands can be expected (large cell and low symmetry). Since we performed our experiments on crystalline aggregates, new bands may also appear because of structural faults, as well as due to morphological effects. For instance, experimental Raman and IR spectra of kaolinite display five bands whereas there are only four modes (Balan et al. 2001). In this case, factor group analysis cannot precisely predict the exact number of hydroxyl peaks displayed in the experimental Raman spectra of each variety. Finally, the O–H-stretching frequency is very sensitive to the occupancy of the surrounding octahedral sites, and especially to the substitution of Mg by Fe (*e.g.* Burns and Strens 1966, in the case of amphiboles). Given the composition of our samples, highest wavenumber bands (near 3690–3700 cm^{-1}) correspond to OH sites coordinated by 3 Mg, and bands corresponding to OH sites coordinated by 2 Mg and 1 Fe should be shifted at lower frequencies by about 15 cm^{-1} (Burns and Strens 1966). Other configurations (1 Mg and 2 Fe, or 3 Fe) are statistically unlikely and the corresponding bands should be very weak. Contributions from OH sites surrounded by Al are also expected (Bancroft and Burns 1969; Strens 1974). Thus, we accepted a number of bands that deals with these considerations but also best fits the spectra (minimum residuals) (Fig. 4).

The OH Raman bands of serpentines are characterized by a contrasting behaviour. We propose that this contrasting pressure behaviour of the O–H-stretching Raman bands is related to the two different types of OH groups. Nevertheless, all but one Raman band in this spectral range display positive shifts as a function of pressure (Figs. 2 and 3). The slight negative shift of one band in the antigorite high-frequency spectrum (−0.9 cm^{-1} GPa^{-1}) is not representative of the behaviour of OH groups, because of the weakness of the peak compared to the whole signal and the absence of this feature in the other serpentine varieties.

Our experimental results are apparently in contradiction with the data obtained by Velde and Martinez (1981). They showed a negative pressure dependence of

the O–H-stretching frequencies on infrared spectra of highly aluminous serpentine (Al = 1.75), close to the amesite end member [$Mg_2Al(SiAl)O_5(OH)_4$]. The authors also found the more pressure-dependent modes to be the O–H-stretching bands around 3440 cm^{-1} which are well developed in infrared spectroscopy for Al-rich serpentines, but are very weak or absent for serpentines close to the Mg end member (Serna et al. 1979). We did not observe these bands in our spectra, due to the small Al content of our samples. The vibrations around 3680 cm^{-1} were found to be about independent of pressure by Velde and Martinez (1981) up to 0.9 GPa. In this limited pressure range, their dataset is not significantly different from ours, given the relatively large errors in the position of IR absorption bands with respect to Raman ones.

The positive shifts we observe may be expected for the inner O4H4 groups, since no hydrogen bonding occurs in these hydroxyl groups (Wicks and O'Hanley 1988). Thus, the positive shifts indicate that the O–H bond is strengthening under compression. Similar positive shifts are observed for OH groups in mica (Holtz et al. 1993), in hydroxyl-clinohumite (Lin et al. 2000) and in chlorite (Kleppe et al. 2003).

Positive shifts were unexpected in the case of the outer OH groups. Indeed, the outer OH groups in serpentine minerals are currently considered to be involved in weak H bonding in order to link adjacent 1:1 layers (*e.g.* Mellini 1982; Wicks and O'Hanley 1988). The high density in hydroxyl groups (one hydrogen atom per 8.2 $Å^2$) compensates the weakness of each interlayer H bonding (Mellini 1982). Compression of the serpentine structure is mostly accommodated by a decrease in the interlayer thickness (Mellini and Zanazzi 1989), which is accompanied by reduced O3···O2 distances and supposedly by increased H bonding (Mellini and Zanazzi 1989; Benco and Smrèok 1998). As far as the O–H-stretching frequency can be considered as a convenient measure of the O–H···O bond strength (*e.g.* Libowitzky 1999), the positive shifts of the O–H symmetric stretching vibrations in serpentine minerals indicate the absence of pressure-induced enhancement of hydrogen bonding. Furthermore, under ambient conditions, only extremely weak hydrogen bonding is inferred from the interlayer O3–H3···O2 bond distances of 3 Å and from O–H-stretching frequencies around 3650 cm^{-1} for lizardite (Mellini 1982; Mellini and Viti 1994), or for antigorite (Mellini et al. 2002). Thus, altogether these observations imply that the interlayer H bonding of serpentine minerals should be considered as extremely weak or absent over the investigated pressure range. This agrees well with the recent Raman results on clinochlore at high pressure by Kleppe et al. (2003). The pressure dependence of all Raman-active O–H-stretching modes of clinochlore is small and positive up to 6 GPa, where a phase transition occurs. Over the same pressure range, the neutron diffraction study of Welch and Marshall (2001) indicates that the main effect of pressure on deuterated clinochlore is a compression of its interlayer achieved by a closure of the O–D···O bond angle (from around 170° at 10^{-4} GPa to 150° at 4.7 GPa), without negligible changes in the O–D and D···O bond length. Alternatively, if we assume that the O–H distance is kept constant, an increase in the O–H···O bond angle could explain the observed positive shifts (Libowitzky 1999). Such a bending might occur if the hydrogen atoms move toward the centre of the six-fold tetrahedral rings (Fig. 1), away from the O_2 and Si, which are moving closer due to the decrease of the interlayer space with pressure.

Toward a new assignment of the symmetric stretching OH vibrations in serpentine minerals

Our study also addresses the still-debated assignment of the OH-stretching modes in serpentine minerals. Structural refinements of lizardite-1*T* from Val Sissone are available (Mellini and Viti 1994; Gregorkiewitz et al. 1996). They indicate that the O4–H4 bond (~0.80 Å) is shorter than the O3–H3 bond (~1.16 Å). According to these data, the outer O3–H3 bonds might be weaker than the inner O4–H4 bonds under room conditions; thus, the contribution of the outer O3–H3 bonds should occur at lower frequency in the Raman spectra, compared to the inner O4–H4 bonds. However, it is commonly assumed that the lower-frequency peaks in the O–H-stretching frequency range correspond to the inner OH groups whereas the higher-frequency peaks are attributed to the vibrations of the outer hydroxyl groups (Kloprogge et al. 1999). Mellini and Zanazzi (1989) have demonstrated that the most important pressure-induced structural change in lizardite occurs along the *c* axis; in this direction, there are only slight variations of the thickness of the layer, while the interlayer thickness is strongly diminishing under compression. The inner OH groups thus shorten, like the surrounding stiff tetrahedral structure, whereas the outer hydroxyl groups are strongly affected by the large reduction of the interlayer thickness. We have previously shown in this paper that there is no enhanced interlayer hydrogen bonding in serpentine. Thus, the outer OH groups can be expected to behave as ionic bonds, whose strength increases with pressure. This leads us to propose a new assignment for the Raman O–H-stretching modes. From this study, we suggest that the more pressure-dependent modes arise from the stretch of outer OH groups whereas the less pressure-sensitive bands, located close to 3700 cm^{-1}, can be assigned to the stretch of inner OH groups. This assignment is in close agreement with the recent *ab initio* calculations of the infrared spectrum of lizardite by Balan et al. (2002), who calculated positions of the IR band due to outer hydroxyl groups at lower frequency than bands due to inner hydroxyl groups.

Acknowledgements The authors are indebted to M. Mellini and A. Baronnet for providing the samples of lizardite-1*T* and polygonal serpentine. Both reviewers are acknowledged for their helpful com-

ments. A.-L. A. is especially grateful to Etienne Balan for enlightening discussions. This work benefited from the support of the French Institut National des Sciences de l'Univers (program Intérieur de la Terre and Centre de spectroscopie in situ at the ENS Lyon).

References

Auzende A-L, Devouard B, Guillot S, Daniel I, Baronnet A, Lardeaux J-M (2002) Serpentinites from Central Cuba : petrology and HRTEM study. Eur J Mineral 14: 905–914

Balan E, Saitta AM, Mauri F, Calas G. (2001) First-principles modeling of the infrared spectrum of kaolinite. Am Mineral 86: 1321–1330

Balan E, Saitta AM, Mauri F, Lemaire C, Guyot F (2002) First-principles calculation of the infrared spectrum of lizardite. Am Mineral 87: 1286–1290

Bancroft GM, Burns RG (1969) Mössbauer and absorption spectral study of alkali amphiboles. Min Soc Am Spec Paper 2: 137–148

Baronnet A, Mellini M, Devouard B (1994) Sectors in polygonal serpentine. A model based on dislocations. Phys Chem Miner 21: 330–343

Benco L, Smrèok L (1998) Hartree-Fock study of pressure-induced strengthening of hydrogen bonding in lizardite-1 T. Eur J Mineral 10: 483–490

Bose K, Ganguly J (1995) Experimental and theoretical studies of the stabilities of talc, antigorite and phase A at high pressures with applications to subduction processes. Earth Planet Sci Lett 136: 109–121

Burns RG, Strens RGJ (1966) Infrared study of the hydroxyl bands in clinoamphiboles. Science 153: 890–892

Fuchs Y, Linares J, Mellini M (1998) Mössbauer and infrared spectrometry of lizardite-1 T from Monte-Fico Elba. Phys Chem Miner 26: 111–115

Gregorkiewitz M, Lebech B, Mellini M, Viti C (1996) Hydrogen positions and thermal expansion in lizardite-1 T from Elba: a low-temperature study using Rietveld refinement of neutron diffraction data. Am Mineral 81: 1111–1116

Guillot S, Hattori K, de Sigoyer J (2000) Mantle wedge serpentinization and exhumation of eclogites: insights form eastern Ladhak northwest Himalaya. Geology 28: 199–202

Irifune T, Kuroda K, Miyajima N (1996) Amorphization of serpentine at high pressure and high temperature. Science 272: 1468–1470

Iwamori H (1998) Transportation of H_2O and melting in subduction zones. Earth Planet Sci Lett 160: 65–80

Kleppe AK, Jephcoat AP, Welch MD (2003) The effect of pressure upon hydrogen bonding in chlorite: Raman spectroscopic study of clinochlore to 26.5 GPa. Am Mineral 88: 567–573

Kloprogge JT, Frost RL, Rintoul L (1999) Single-crystal Raman microscopic study of the abestos mineral chrysotile. Phys Chem Chem Phys 1: 2559–2564

Lemaire C, Guyot F, Reynard B (1999) Vibrational spectroscopy (IR and Raman) of OH groups in chrysotile lizardite and antigorite. European Union of Geosciences 10, Strasbourg, pp 654

Libowitzky E (1999) Correlation of O–H-stretching frequencies and O···H–O hydrogen bond lengths in minerals. Mh Chemie 130: 1047–1059

Lin CC, Liu LG, Mernagh TP, Irifune T (2000) Raman spectroscopic study of hydroxyl–clinohumite at various pressure and temperature. Phys Chem Miner 27: 320–331

Mao HK, Xu J, Bell PM (1986) Calibration of the ruby pressure gauge to 800 kbar under quasi-hydrostatic conditions. J Geophys Res 91: 4763–4767

Meade C, Jeanloz R (1991) Deep-focus earthquakes and recycling of water into the Earth's mantle. Science 252: 68–72

Mellini M, Zanazzi PF (1989) Effects of pressure on the structure of lizardite 1 T. Eur J Mineral 1: 13–19

Mellini M, Viti C (1994) Crystal structure of lizardite-1 T from Elba Italy Am Mineral 79 1194–1198

Mellini M, Trommsdorff V, Compagnoni R (1987) Antigorite polysomatism: behaviour during progressive metamorphism. Contrib Mineral Petrol 97: 147–155

Mellini M, Fuchs Y, Viti C, Lemaire C, Linarès J (2002) Insights into the antigorite structure from Mössbauer and FTIR spectroscopies. Eur J Mineral 14: 97–104

Scambelluri M, Müntener O, Hermann J, Piccardo GB, Trommsdorff V (1995) Subduction of water in the mantle: history of an alpine peridotite. Geology 23: 459–462

Schmidt MW, Poli S (1998) Experimentally based water budget for dehydrating slabs and consequences for arc magma generation. Earth Planet Sci Lett 163: 361–379

Serna CJ, White JL, Velde BD (1979) The effect of aluminum on the infrared spectra of 7 angström trioctahedral minerals. Mineral Mag 43: 141–148

Strens RGJ (1974) The common chain, ribbon and ring silicates. In: FarmerVC (ed) The infrared spectra of minerals, Mineralogical Society London, pp 305–330

Uehara S (1998) TEM and XRD study of antigorite superstructures. Can Mineral 36: 1595–1605

Ulmer P, Trommsdorff V (1995) Serpentine stability to mantle depths and subduction-related magmatism. Science 268: 858–861

Velde B, Martinez G (1981) Effect of pressure on OH-stretching frequencies in kaolinite and ordered aluminous serpentine. Am Mineral 66: 196–200

Viti C, Mellini M (1997) Contrasting chemical compositions in associated lizardite and chrysotile in veins from Elba, Italy. Eur J Mineral 9: 585–596

Welch MD, Marshall WG (2001) High-pressure behavior of clinochlore. Am Mineral 86: 1380–1386

Wicks FJ, O'Hanley D (1988) Serpentine minerals: structure and petrology. In: Bailey SW (ed) Hydrous phyllosilicates, vol 19. Reviews in Mineralogy, Mineralogical Society of America, Washington DC, pp 91–167

Wicks FJ, Whittaker EJM (1970) Chemical differences among the serpentine 'polymorphs'; a discussion. Am Mineral 55: 1025–1074

Wunder B, Schreyer W (1997) Antigorite: high-pressure stability in the system $MgO–SiO_2–H_2O$ (MSH). Lithos 41: 213–227